NEURONAL ELECTRICAL ACTIVITY, ENERGY CONSUMPTION AND MITOCHONDRIAL ATP RESTORATION DYNAMICS: A PHYSIOLOGICAL BASED MODEL FOR FMRI

Rita Gafaniz and J. Miguel Sanches

Institute for Systems and Robotic / Instituto Superior Técnico
Lisbon, Portugal

ABSTRACT

fMRI is a widely used method to detect the activated brain regions due to a stimulus application. Commonly, it employs the BOLD contrast, which is based on the correlation between physiological function, energy metabolism and haemodynamics. However, the BOLD signal is weak and noisy, so that, an accurate mathematical model to describe the *Haemodynamic Response Function* (HRF) to activation is needed.

In this paper, a physiologically-based model relating energy metabolism with the corresponding neuronal electrical activity (NEA) is proposed. This model is an extension of a previous one that couples ATP consumption with the NEA. Decreased ATP levels inside the neuron increase the metabolic rate. Here, the mitochondria play a central role. It is modeled as a classical regulator to maintain ATP *homeostasis*.

The main transfer function, a second-order linear system, is able to describe the physiological mechanisms involved in the neuronal activity and is useful to model the overall HRF.

Index Terms— Neuro-Metabolic Model, BOLD, fMRI

1. INTRODUCTION

Functional Magnetic Resonance Imaging (fMRI) has being used worldwide as a powerful neuroscientific research technique to study the neural basis of human cognition. fMRI measurements can be accomplished by different techniques, but the *Blood-Oxygenation-Level-Dependent* (BOLD) technique is the most frequently used. Without making direct measurements on the neuronal activity, these approaches take advantage of neuro-metabolic and neuro-vascular physiological events, accompanying brain activation, that locally change the diamagnetic oxygen (O_2), namely *Cerebral Metabolic Rate of Oxygen* ($CMRO_2$), *Cerebral Blood Flow* (CBF) and *Cerebral Blood Volume* (CBV). This set of physiological responses are referred as the *Haemodynamic Response Function* (HRF). Nevertheless, retrieval of this information is a challenging problem, not only because BOLD signal changes are very small, but also due to the corrupting noise in fMRI data, which affects the brain activity detection sensitivity. Thus, an accurate model that predicts the HRF evoked by a given stimuli is needed.

Fig.1 displays the main components involved in the relation of the neuronal electrical activity (NEA), $r(t)$, with the measured HbO_2/Hb. The majority of the energy expended in the brain is spent on signaling and most of that energy is employed by neurons, particularly by the *sodium/potassium pump* (Na/K-ATPase), to reverse the ionic fluxes caused by NEA. Therefore, the ATP consumption, $ATP_r(t)$, is mainly due to the Na/K-ATPase activity. Decreased ATP levels inside the neuron stimulates the metabolic pathways that restores it [1]. ATP is regenerated mainly via the oxidative metabolism of glucose (Glc), which is accomplished via glycolysis (Gly) and mitochondrial respiration. This last pathway is responsible for almost the entire O_2 consumption (i.e. $CMRO_2$) [2] in the central nervous system [3], thus, it represents a critical determinant of the BOLD signal. O_2 and Glc diffuse from the vasculature into the cell. Moreover, ATP consumption and energy metabolism stimulate the release of vasodilators, for instance Adenosine (A) and Nitric Oxide (NO), leading to increased blood flow and venous dilatation [4]. The signal measured by BOLD fMRI experiments, i.e. HbO_2/Hb, is derived from the combination of the dynamic changes of $CBF(t)$, $CBV(t)$ and $CMRO_2(t)$ in local capillary and venous blood.

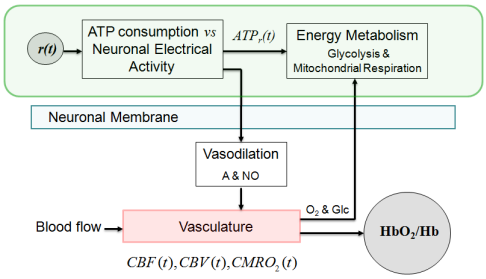

Fig. 1. A physiologically-based model design for the HRF.

In this paper, it is proposed a linear model for the coupling between the NEA and energy metabolism, a *Neuro-Metabolic Model* (NMM). The NMM is an extension of a previous model that links ATP consumption rate with the NEA [5]. The *Na/K-ATPase* is an important element because its ATP consumption directly links electrophysiological features to energy metabolism. The ATP synthesis is here assumed to be solely made by the *mitochondria*, which act as a regulator in a Control Theory perspective.

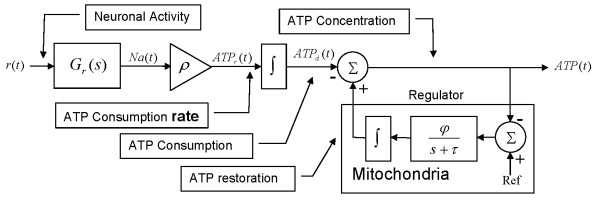

Fig. 2. Neuro-Metabolic Model overview.

Partially supported by project the FCT (ISR/IST plurianual funding) through the PIDDAC Program funds and FCT project "'Detection of Brain Microstates in Fibromyalgia"' (PTDC/SAU-BEB/104948/2008)

2. MODEL DESCRIPTION

The NMM is composed by two major dynamic systems, as shown in Fig.2. The first, presented in [5], relates the NA with the ATP consumption and the second, proposed here, describes the ATP synthesis by the *mitochondria* (the main energy plant of the cell). In this model the intracellular ATP concentration, denoted by ATP, is a resource that is expended mostly to restore Na^+ and K^+ *homeostasis* (that were degraded due to the electrophysiological processes associated with the NEA), and is restored mainly via mitochondrial respiration. The *mitochondria* act as a regulator, according with the Control Theory [6], continuously sensing the ATP concentration inside the neuron, while adjusting its activity in order to restore ATP into a biological predefined reference level, i.e. maintain ATP *homeostasis*. The dynamic evolution of the intracellular ATP concentration along the time, $ATP(t)$, results from the contribution of these two processes. The mathematical formulation of both processes, which is presented in the next sections, is based on linear ordinary differential equations with constant coefficients which corresponds, from a System Theory point of view, to a *Linear Time-Invariant* (LTI) system [6].

The Laplace Transform (*LT*) [6] of the ATP consumption along the time (see Fig.2), is given by the following expression

$$ATP_d(s) = \frac{1}{s} ATP_r(s) = \frac{\rho}{s} Na(s), \tag{1}$$

where $ATP_r(s)$ is the *LT* of the ATP consumption rate and $Na(s)$ is the *LT* of the intracellular concentration of sodium, Na, whose expression is [5]

$$Na(s) = G_N(s)Na_e + G_K(s)K_e + G_r(s)R(s), . \tag{2}$$

Na_e and K_e are the extracellular concentrations of Na^+ and K^+, respectively, and $R(s)$ is the *LT* of the NEA, $r(t)$. The Transfer Functions (TFs) $G_N(s)$, $G_K(s)$ and $G_r(s)$are second-order systems (two poles) with a zero

$$G_N(s) = \frac{\eta_1 s + \eta_2}{s^2 + \psi_1 s + \psi_2}, \tag{3}$$

$$G_K(s) = \frac{\eta_3 s + \eta_4}{s^2 + \psi_1 s + \psi_2}, \tag{4}$$

$$G_r(s) = \frac{\eta_5 s + \eta_6}{s^2 + \psi_1 s + \psi_2}, \tag{5}$$

$$\tag{6}$$

The mitochondrial activity, represented at the right side of Fig.2, is modeled by a classical regulator according the Control Theory, as shown in Fig.3. In this perspective, the *mitochondria* act as a regulator [7], continuously sensing the ATP concentration and maintaining it at a predefined biological reference level, Ref, against external disturbances, such as the ATP consumed by the *Na/K-ATPase*, i.e. ATP_d. In particular, the *mitochondria* are modeled as a second order linear system with the pole at the origin. The system with this pole, obtained with an output integrator, is a *type-I* system [6] where the steady-state error to the step is zero and finite to the ramp.

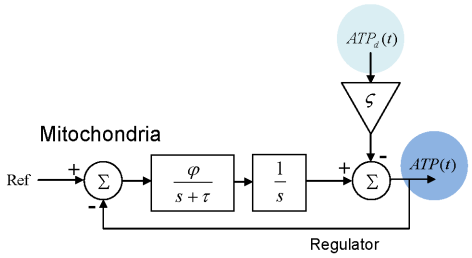

Fig. 3. The Simulink model of the mitochondria: a type-1 regulator that maintains the intracellular concentration of ATP ($ATP(t)$).

By taking into account (1), the TF of the overall ATP inside the neuron is

$$ATP(s) = \frac{\varphi}{s^2 + \tau s + \varphi} Ref - \frac{(s+\tau)\zeta\rho}{s^2 + \tau s + \varphi} Na(s). \tag{7}$$

By applying equation (1) and (2) to equation (7), and after some straightforward manipulations, the TF relating $ATP(t)$ with the corresponding Ref, Na_e, K_e and $r(t)$ is given by

$$\begin{aligned} ATP(s) &= L_R(s)Ref(s) + L_N(s)Na_e(s) + \\ &\quad L_K(s)K_e(s) + L_r(s)R(s), \end{aligned} \tag{8}$$

where the functions $L_R(s)$, $L_N(s)$, $L_K(s)$ and $L_r(s)$ are the following fourth-order systems (four poles) with two zeros

$$L_R(s) = (\lambda_1 s^2 + \lambda_2 s + \lambda_3)/D(s), \tag{9}$$

$$L_N(s) = (\lambda_4 s^2 + \lambda_5 s + \lambda_6)/D(s), \tag{10}$$

$$L_K(s) = (\lambda_7 s^2 + \lambda_8 s + \lambda_9)/D(s), \tag{11}$$

$$L_r(s) = (\lambda_{10} s^2 + \lambda_{11} s + \lambda_{12})/D(s). \tag{12}$$

where $D(s) = (s^2 + \psi_1 s + \psi_2)(s^2 + \psi_3 s + \psi_4)$. The coefficients are defined in Table 1.

Table 1. Coefficients of $ATP(s)$

Parameters
$\lambda_1 = \varphi$
$\lambda_2 = \varphi.\psi_1$
$\lambda_3 = \varphi.\psi_2$
$\lambda_4 = -\rho.\zeta.\eta_1$
$\lambda_5 = -\rho.\zeta.(\tau.\eta_1 + \eta_2)$
$\lambda_6 = -\rho.\zeta.\tau.\eta_2$
$\lambda_7 = -\rho.\zeta.\eta_3$
$\lambda_8 = -\rho.\zeta.\tau.\eta_3$
$\lambda_9 = 0$
$\lambda_{10} = -\rho.\zeta.\eta_5$
$\lambda_{11} = -\rho.\zeta.(\tau.\eta_5 + \eta_6)$
$\lambda_{12} = -\rho.\zeta.\tau.\eta_6$
$\psi_3 = \tau$
$\psi_4 = \varphi$

2.1. Mitochondria Parameters

The poles of the second order regulator that models the mitochondrial activity are the roots of the characteristic equation of the *mitochondria*

$$s^2 + \tau.s + \varphi = 0 \leftrightarrow s = \frac{-\tau \pm \sqrt{\tau^2 - 4\varphi}}{2}. \tag{13}$$

where the lowest frequency pole (the one closest to the origin) is the reciprocal of the *mitochondria* time constant, reported in the litera-

ture [8] as being $30s$. Therefore,

$$p_1 = \frac{-\tau + \sqrt{\tau^2 - 4\varphi}}{2} = -1/30 \leftrightarrow \tau = 30\varphi + 1/30. \quad (14)$$

The predefined biological reference value, Ref, is obtained from the steady state solution of equation (7) by using the final value theorem [6] and the previously referred equilibrium values: i) $Na = 15$ mM, and ii) $ATP = 2.2$ mM [9,10],

$$Ref = ATP + \frac{\rho.\zeta.\tau}{\varphi} Na. \quad (15)$$

The selection of the parameters φ and ζ were performed in a trial and error basis in order to obtain the simulation results that better fits the experimental data [10]. Furthermore, it was observed a low sensitivity of the result to the φ parameter. The selected values for these parameters are $\zeta = 0.12$ and $\varphi = 1$. Hence, from equation (14), $\tau \simeq 30\text{s}^{-1}$ and from equation (15), $Ref \simeq 2.7748$mM.

Table 2 lists the TF coefficients defined in equations (2) and (8).

Table 2. Coefficients of the Transfer Functions

Coefficients	
η_1 = 0.26 s^{-1}	λ_6 = -7.62×10^{-5} s^{-4}
η_2 = 0.002 s^{-2}	λ_7 = -3.33×10^{-4} s^{-1}
η_3 = 0.26 s^{-1}	λ_8 = -0.01 s^{-3}
η_4 = 0	λ_9 = 0
η_5 = 23 $mMs^{-1}V^{-1}$	λ_{10} = -0.03 $mMs^{-2}V^{-1}$
η_6 = 14.92 $mMs^{-2}V^{-1}$	λ_{11} = -0.90 $mMs^{-3}V^{-1}$
λ_1 = 1	λ_{12} = -0.57 $mMs^{-4}V^{-1}$
λ_2 = 0.68 s^{-1}	ψ_1 = 0.68 s^{-1}
λ_3 = 0.02 s^{-2}	ψ_2 = 0.02 s^{-2}
λ_4 = -3.37×10^{-4} s^{-2}	ψ_3 = 30 s^{-1}
λ_5 = -0.01 s^{-3}	ψ_4 = 1

3. RESULTS

In this section, the NMM model, displayed in Fig.2 and described by equation (8), is simulated with typical stimuli and the results are compared with the ones described in the literature [10].

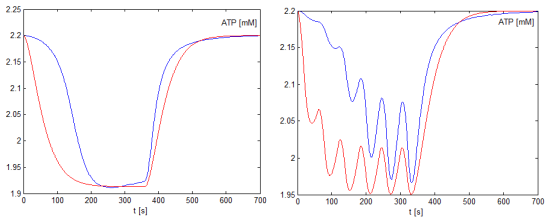

(a) (b)

Fig. 4. ATP dynamics for a sustained activation (a) and a repetitive activation (b). The results obtained with the NMM (in red) are compared with [10] (in blue).

Fig.4 displays the time course of ATP in the case of a sustained activation (see Fig.4(a)), where $r(t)$ is a given sequence of pulses ($A = 0.1$V, $b = 1$ms, $f = 100$Hz) for $0 \leq t \leq 360$, and in the case of a repetitive activation (see Fig.4(b)), where $r(t)$ consists of six cycles of stimulation with a sequence of pulses ($A = 0.1$V, $b = 1$ms, $f = 230$Hz) for a time duration of 20s, followed by 40s without stimuli. There is some discrepancy between the results obtained with the NMM (in red) and those obtained by [10] (in blue), specially at the beginning of the simulation. The HRF model proposed by [10] is based on fourteen nonlinear differential equations, whereas the model proposed here is a second order linear model. In particular, the balance equation for ATP dynamics derived by [10] is affected by several processes, depending on several parameters and variables. Since the NMM is linear and it is modelled focusing the most relevant processes, according to the literature, such differences between these responses are expected. However, at the end of the simulation, the rate constant for ATP recovery has a good agreement with [10].

Despite the $ATP(s)$ (see Eqn. (8)) is a fourth-order system, the curves of Fig.4 (in red) resemble a typical response of a second-order system. The pole-zero map of the TF relating $ATP(t)$ with $r(t)$, $L_r(s)$, is displayed in Fig.5 and supports this observation. The

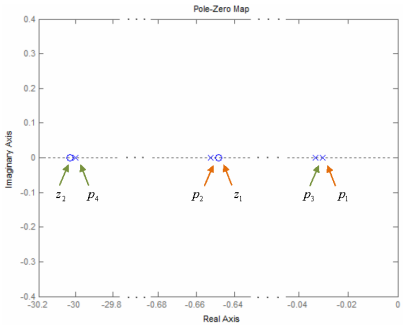

Fig. 5. Pole-zero map of $L_r(s)$. The orange arrows indicate the poles and zeros from the Na/K-ATPase and the green ones indicate those from the mitochondria.

zeros are $z_1 = -0.65$ rads^{-1} and $z_2 = -30.03$ rads^{-1}, whereas the poles are $p_1 = -0.031$ rads^{-1}, $p_2 = -0.653$ rads^{-1}, $p_3 = -0.033$ rads^{-1} and $p_4 = -30.00$ rads^{-1}. Hence, z_1 cancels the effect of p_2 and z_2 cancels the effect of p_4. Therefore, there is a dominant pole condition, performed by the poles p_1 and p_3, and $L_r(s)$ can be simplified to a second-order system with two poles (p_1 and p_3) and no zeros

$$L_r(s) \approx \frac{\Psi_0}{(s - p_1)(s - p_3)}, \quad (16)$$

where $\Psi_0 = \frac{\lambda_{12} p_1 p_3}{\psi_2 \psi_4}$ and p_1 and p_3 are given by the following expressions

$$p_1 = \frac{-\psi_1 + \sqrt{\psi_1^2 - 4\psi_2}}{2}, \quad (17)$$

$$p_3 = \frac{-\tau + \sqrt{\tau^2 - 4\varphi}}{2}, \quad (18)$$

and where $\psi_1 = \alpha_N + \gamma_K + 3\rho - \beta_N - \delta_K$ and $\psi_2 = (\alpha_N - \beta_N + 3\rho).(\gamma_K + \delta_K) - \beta_N.(\delta_K + 2\rho)$.

By taking into account that $\psi_1^2 >> -4\psi_2$ and $\tau^2 >> -4\varphi$, Eqn. (17) and (18) can be simplified if the *Taylor Series Expansion* is applied as follows

$$\sqrt{\psi_1^2 - 4\psi_2} \approx \sqrt{\psi_1^2} + \frac{(\psi_1^2)^{-1/2}}{2}(-4\psi_2) = \psi_1 - \frac{2\psi_2}{\psi_1},$$

$$\sqrt{\tau^2 - 4\varphi} \approx \sqrt{\tau^2} + \frac{(\tau^2)^{-1/2}}{2}(-4\varphi) = \tau - \frac{2\varphi}{\tau}. \quad (19)$$

Therefore, $p_1 \approx -\frac{\psi_2}{\psi_1}$ and $p_3 \approx -\frac{\varphi}{\tau}$. Moreover, ψ_1 and ψ_2 depend on several constants, whose values are $\alpha_N = 0.0026\text{s}^{-1}$, $\beta_N = -0.2612\text{s}^{-1}$, $\gamma_K = 0.0038\text{s}^{-1}$, $\delta_K = -0.3835\text{s}^{-1}$, $3\rho = 0.0319\text{s}^{-1}$ and $2\rho = 0.0213\text{s}^{-1}$. Since some of these terms are much smaller than others, after some simplifications and straightforward arrangements, the first pole is

$$p_1 \approx -3\rho + \xi, \tag{20}$$

where $\xi = \frac{\beta_N \rho - \alpha_N \delta_K - \beta_N \gamma_K}{\beta_N + \delta_N} = 0.0012$. This means that p_1 mainly depends on ρ, the *Na/K-ATPase* activity time constant.

The similarity between p_1 and p_3 allows to simplify the TF in equation (16) by using the following second-order system with a double pole

$$L_r(s) \approx \frac{\Psi}{(s-p)^2}, \tag{21}$$

where $\Psi = \frac{\lambda_{12} p^2}{\psi_2 \psi_4}$ and $p = (p_1 + p_3)/2 = -0.0320\text{rads}^{-1}$, which corresponds to the mean value of the simplified $p_1 \approx -0.0307\text{rads}^{-1}$ and $p_3 \approx -0.0333\text{rads}^{-1}$.

Finally, after the overall approximations, $ATP(s)$ is given by the following expression

$$\begin{aligned} ATP(s) \quad = \quad & \frac{\lambda_3}{\psi_2 \psi_4} Ref(s) + \frac{\lambda_6}{\psi_2 \psi_4} Na_e(s) + \\ & \frac{\lambda_9}{\psi_2 \psi_4} K_e(s) + \frac{\lambda_{12} p^2}{\psi_2 \psi_4} \frac{1}{(s-p)^2} R(s). \end{aligned} \tag{22}$$

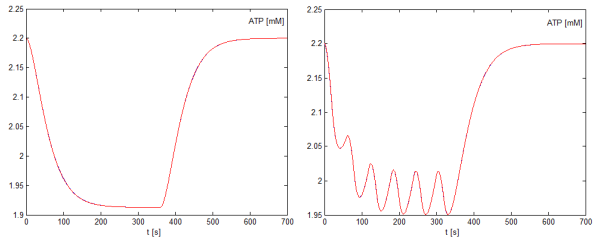

(a) (b)

Fig. 6. Comparison between the fourth order $ATP(s)$ (in blue) with second order $ATP(s)$ (in red) for a sustained activation (a) and a repetitive activation (b).

Fig.6 displays a comparison between the fourth-order system presented in equation (8) (in blue) and the second-order system (with double poles) of equation (22) (in red) for a sustained activation (Fig.6(a)) and a repetitive activation (Fig.6(b)). The superposition of the curves shows the feasibility of this approximation.

The Bode diagram of $L_r(s)$, defined in Eqn. (21), is displayed in Fig.7. In this diagram it is also represented the harmonic components of the neuronal activity, modeled as a comb of Diracs with a typical frequency of $f = 100Hz$. As it can be seen, the final TF, which is dominated by the large *Na/K-ATPase* and *mitochondria* time constants, is a low-pass filter ($\omega_c = 0.032rads^{-1}$), removing all components of the NA except the DC one (0 Hz). This means that the exact shape of the AP, defined by its high order harmonics, is not relevant for the computation of the ATP dynamics, so that, the ATP dynamics is essentially related with the mean value of the NA, rather than its specific shape, as referred in [11].

Thus, the input is essentially characterized by the pulse density, or equivalently, by its frequency and the shape of action potentials

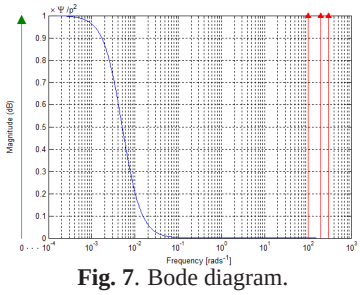

Fig. 7. Bode diagram.

are meaningless.

4. CONCLUSIONS

In this paper, a new physiologically-based mathematical model describing the neuronal electrical activity, $r(t)$, and the intracellular ATP dynamics, $ATP(t)$, is presented. The results obtained with the proposed Neuro-Metabolic Model (NMM) are compared with those obtained from other state of the art model, described in the literature. The time constants for Na and ATP recovery after the stimulus show a good agreement with [10]. Differences to the other model are justified by the simplifications adopted in the design of the proposed model in order in order to make it possible its inclusion in an larger model describing the *Haeomodynamic Response Function* (HRF) generation process used in *functional Resonance Magnetic Imaging* (fMRI).

5. REFERENCES

[1] M. Mata, D. J. Fink, H. Gainer, C. B. Smith, L. Davidsen, H. Savaki, W. J. Schwartz, and L. Sokoloff, "Activity-dependent energy metabolism in rat posterior pituitary primarily reflects sodium pump activity," *Journal of Neurochemistry*, vol. 34, pp. 213–215, January 1980.

[2] Louis Sokoloff, "The physiological and biochemical bases of functional brain imaging," *Cognitive Neurodynamics*, vol. 2, pp. 1–5, 2008.

[3] Adelbert Ames, "CNS energy metabolism as related to function," *Brain Research Reviews*, vol. 34, pp. 42–68, 2000.

[4] Fernando Costa and Italo Biaggioni, "Role of nitric oxide in adenosine-induced vasodilation in humans," *Hypertension*, vol. 31, pp. 1061–1064, 1998.

[5] Rita Gafaniz and João Sanches, "ATP consumption and neural electrical activity: A physiological model for brain imaging," in *Engineering in Medicine and Biology Society, 2010. EMBS 2010. 32th Annual International Conference of the IEEE*, September. 2010.

[6] Alan V. Oppenheim, Alan S. Willsky, and Syed Hamid Nawab, *Signals & Systems*, Prentice Hall, 1996.

[7] Bernard Korzeniewski, "Regulation of ATP supply in mammalian skeletal muscle during resting state → intensive work transition," *Biophysical Chemistry*, vol. 83, pp. 19–34, 2000.

[8] Brian Glancy, Thomas Barstow, and Wayne T. Willis, "Linear relation between time constant of oxygen uptake kinetics, total creatine, and mitochondrial content in vitro," *Cell Physiology*, vol. 17, pp. 79–87, 2007.

[9] Jaakko Malmivuo and Robert Plonsey, Eds., *Bioelectromagnetism, Principles and Applications of Bioelectric and Biomagnetic Fields*, Oxford University Press, 1995.

[10] Agnés Aubert and Robert Costalat, "A model of the coupling between electrical activity, metabolism, and hemodynamics: Application to the interpretation of functional neuroimaging," *Neuroimage*, vol. 17, pp. 1162–1181, 2002.

[11] Peter Dayan and L. F. Abbott, Eds., *Theoretical Neuroscience: Computational and Mathematical Modeling of Neural Systems*, MIT Press, 2001.